Sensitivity of ocean circulation and sea-ice conditions to loss of West Antarctic ice shelves and ice sheet

Marion BOUGAMONT,[1*] Elizabeth C. HUNKE[2], Slawek TULACZYK[1]

[1]*Department of Earth and Planetary Sciences, University of California, Santa Cruz, California 95064, USA*
E-mail: tulaczyk@pmc.ucsc.ed
[2]*T-3 Fluid Dynamics Group, Los Alamos National Laboratory, Los Alamos, New Mexico 87545, USA*

ABSTRACT. We use a global coupled ocean–sea ice model to test the hypothesis that the disintegration of the West Antarctic ice sheet (WAIS), or just its ice shelves, may modify ocean circulation and sea-ice conditions in the Southern Ocean. We compare the results of three model runs: (1) a control run with a standard (modern) configuration of landmask in West Antarctica, (2) a no-shelves run with West Antarctic ice shelves removed and (3) a no-WAIS run. In the latter two runs, up to a few million square kilometres of new sea surface area opens to sea-ice formation, causing the volume and extent of Antarctic sea-ice cover to increase compared with the control run. In general, near-surface waters are cooler around Antarctica in the no-shelves and no-WAIS model runs than in the control run, while warm intermediate and deep waters penetrate further south, increasing poleward heat transport. Varying regional responses to the imposed changes in landmask configuration are determined by the fact that Antarctic polynyas and fast ice develop in different parts of the model domain in each run. Model results suggest that changes in the extent of WAIS may modify oceanographic conditions in the Southern Ocean.

INTRODUCTION

There is an ongoing scientific discussion about the potential short-term (in)stability of the marine-based West Antarctic Ice Sheet (WAIS) (Bentley, 1997, 1998; Bindschadler, 1997, 1998; Oppenheimer, 1998). Geological evidence suggests that the WAIS collapsed at least once during the Quaternary (Scherer and others, 1998). Decline of the WAIS would expose up to a few million square kilometres of new sea surface area to extreme polar climate. Processes associated with sea-ice formation, such as brine rejection, could modify regional and global thermohaline circulation. Moreover, the complete disintegration of the WAIS would open a new seaway through the West Antarctic.

Current global ocean circulation models typically treat Antarctica as any other continent, with a fixed land mask (McClean and others, 1997; Best and others, 1999; Goosse and Fichefet, 1999). Using a coupled ocean–sea ice model developed at Los Alamos National Laboratory (LANL), we compare results of three spin-up experiments under similar initial and atmospheric conditions (with modified geometric configurations) in West Antarctica. This comparison demonstrates that Southern Ocean sea-ice conditions and ocean circulation may be modified by changes in the extent of West Antarctic ice shelves and ice sheet. These modelling results may aid future studies focused on the stability of the WAIS by providing guidance regarding potential feedbacks between its retreat and proximal sea-ice and ocean conditions. Our results may also be helpful in the interpretation of marine and ice-core records of paleoenvironmental conditions in the region during past periods of WAIS reduction or absence (e.g. Scherer and others, 1998).

Due to several limitations in the experimental setting, we do not attempt to predict the Southern Ocean circulation pattern during or after disintegration of the ice shelves and/or the WAIS, and the results presented here are not meant to be quantitatively precise. Rather, we focus on the qualitative direction of the trends observed in the different scenarios in response to modified sea-ice production.

METHODS

The set of numerical experiments described here represents, to our knowledge, the first systematic attempt to assess the oceanographic consequences of changes in the extent of West Antarctic ice masses. This preliminary study faces some practical limitations on the length of model runs (detailed below) and physical veracity of available modelling tools. Our work represents a typical perturbation experiment, in which we compare two test runs (referred to as 'no-shelves' and 'no-WAIS') to a control run with a standard landmask.

Models

The ocean model used in this study is the Parallel Ocean Program (POP) (Smith and others, 1992), which runs on a 100×116, $\sim 3^\circ$ resolution global grid, with 25 ocean depth levels (Fig. 1). The ocean model is coupled to the Los Alamos climate ocean and sea-ice model (CICE), a dynamic-thermodynamic sea-ice model fully described in the documentation and software user's manual (Hunke and Lipscomb, 2001). CICE shares the $\sim 3^\circ$ horizontal grid with the ocean model. POP does not include treatment of sub-ice-shelf cavity circulation.

POP and CICE are coupled via the National Center for Atmospheric Research (NCAR) Community Climate System Model (CCSM) coupler (cpl5). The CCSM also incorporates full atmosphere and land models (Blackmon and others, 2001), in place of which we are using data models that read forcing data from files (e.g. the land model provides monthly river runoff data). The quantities computed by the ocean

*Present address: Bristol Glaciology Centre, School of Geographical Sciences, University of Bristol, Bristol BS8 1SS, UK.

https://doi.org/10.3189/002214307783258440 Published online by Cambridge University Press

code and transferred to the sea-ice model include sea surface temperature, salinity, currents and a freezing or melting potential. The atmospheric data provided by the flux coupler to the sea-ice model include the air potential temperature, shortwave radiation, incoming longwave radiation and precipitation rate. In return, the sea-ice model provides to the coupler sensible and latent heat flux, outgoing longwave radiation, evaporated water flux, surface albedo, surface temperature, penetrating shortwave radiation, freshwater flux and net heat flux to the ocean. These lists are non-exhaustive and include only the most important parameters. Additional information about the POP–CICE coupled model can be found in Prasad and others (2005).

Atmospheric forcing

We use a 10 year cycle of atmospheric forcing data, 1979–88, which includes temperature, humidity, density and wind every 6 hours from the National Center for Environmental Prediction, monthly International Satellite Cloud Climatology Project shortwave and cloud fraction, and monthly microwave sounding unit precipitation (Xie and Arkin, 1996).

The biggest challenge with atmospheric forcing arises in the parts of West Antarctica where shelf and land ice are removed in experimental runs to expose new sea surface area. Due to limited computational time, we do not use a fully coupled atmosphere–ocean model, but rather implement a simpler atmospheric mixed-layer model (Seager and others, 1995). This model computes exchange coefficients for heat, moisture and momentum fluxes that take into account the modelled ocean surface temperature, atmospheric diffusion and advection: notably advection of continental air mass properties over the ocean surface. Hence, the model has a weak coupling between the evolution of ocean surface variables and some of the atmospheric variables. However, wind is not included in the treatment of Seager and others (1995) and is part of prescribed climatic forcing. Therefore, wind strength and direction do not evolve as we change ice extent in West Antarctica.

To test the sensitivity of our results to different assumptions about atmospheric forcing, we also ran experiments using fully prescribed atmospheric conditions. Detailed comparison of the runs with different atmospheric forcing is beyond the scope of this paper. A general comparison indicates that introduction of the mixed-layer treatment has significant effects on atmospheric boundary conditions in the areas where ice is removed in experimental runs. However, the impact of this treatment on circum-Antarctic and global aspects of the model output is negligible. We prefer the mixed-layer treatment because it is able to adjust atmospheric parameters to the removal of ice specified in our numerical experiments. It also has one additional benefit, discussed in the following section.

Landmask and bathymetry

We modify the ocean bathymetric grid so that the Ross Ice Shelf (RIS), the Filchner–Ronne Ice Shelf (FRIS) and/or WAIS are treated as part of the global ocean (Fig. 1). To obtain the bathymetry in the regions where ice was removed, we use the BEDMAP digital topography/bathymetry dataset (Lythe and others, 2001). The standard grid configuration (Fig. 1a) is used in the control run of POP–CICE. A global grid whose landmask simulates the removal of the RIS and FRIS is used for the no-shelves run, as shown in Figure 1b. Finally, the WAIS is removed in the third configuration (no-WAIS run,

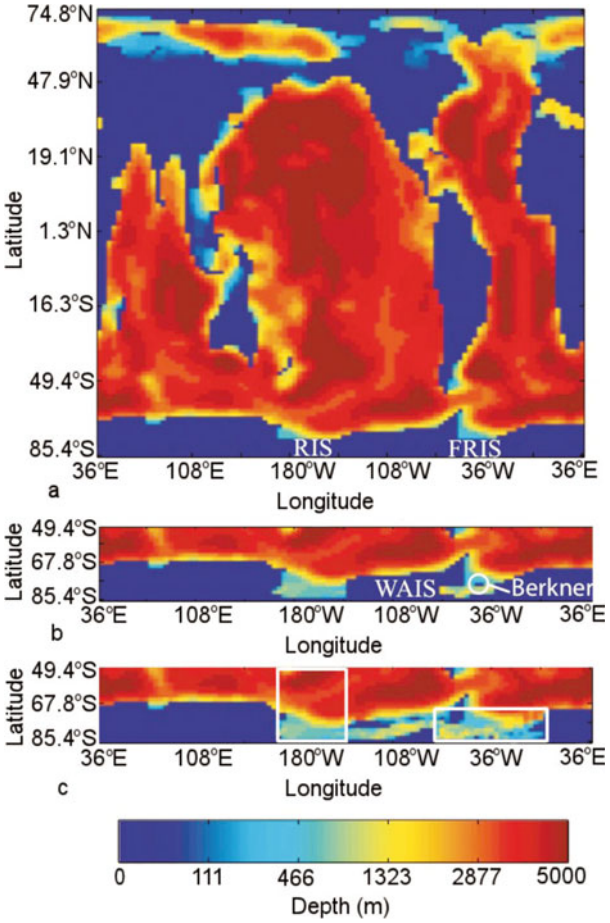

Fig. 1. Bathymetric grids used in the different experiments: (a) global grid from the control run; (b) southern portion of the global grid in which Ross Ice Shelf (RIS) and Filchner–Ronne Ice Shelf (FRIS) have been removed, referred to as the no-shelves run; (c) the no-WAIS grid; as in (b) but with the entire West Antarctic ice sheet removed. The white circle in (b) marks the location of Berkner Island and the two white rectangles locate the RIS and FRIS areas.

Fig. 1c). In the latter case, we do not correct the bathymetry for glacioisostatic uplift due to ice sheet removal. After full equilibration (~10 000 years) this uplift should reach a few hundred metres, with ~6 m of sea-level rise due to the melted ice sheet. We ignore the impact of both isostatic rebound and altered sea level on configuration of the coastline, ocean depth and sea-water freshening, discussed further in the section on selected model limitations.

Initial conditions

The ocean salinity and temperature were extrapolated from World Ocean Atlas data (Levitus and others, 1994a, b) onto land and then interpolated onto each grid, including the areas exposed by removal of West Antarctic ice shelves and ice sheet. The initial velocities in the ocean are equal to zero everywhere. The initial conditions for the sea-ice model were produced by running the ice model in a stand-alone mode, forced with the atmosphere data from 1992–96. The stand-alone sea-ice model uses a slab-ocean mixed-layer model for ice–ocean heat fluxes, and begins from slab-ice conditions identical in each case.

With a time step of 1 hour for both the ocean model and the sea-ice model, running POP–CICE for ~40 model years

https://doi.org/10.3189/002214307783258440 Published online by Cambridge University Press

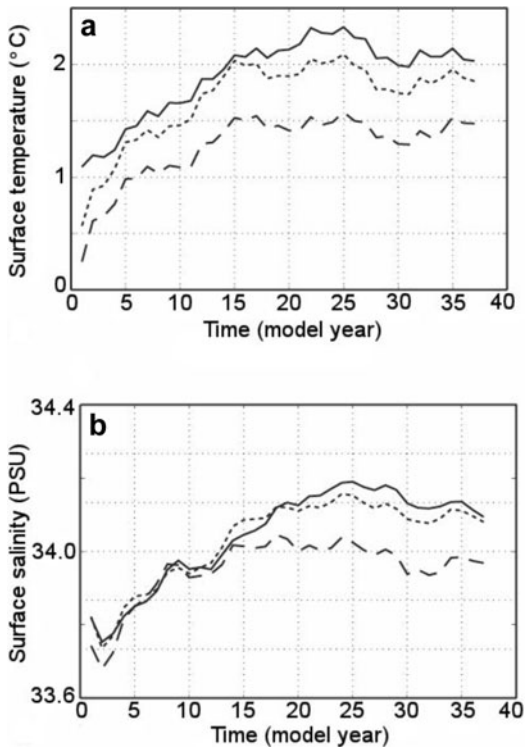

Fig. 2. Time series showing (a) spatially averaged ocean surface temperature and (b) salinity. Monthly values are averaged across the southern high latitudes (84° S to 49.4° S) and all longitudes. The control run is shown with the solid lines, the no-shelves run with dotted lines and the no-WAIS run with dashed lines.

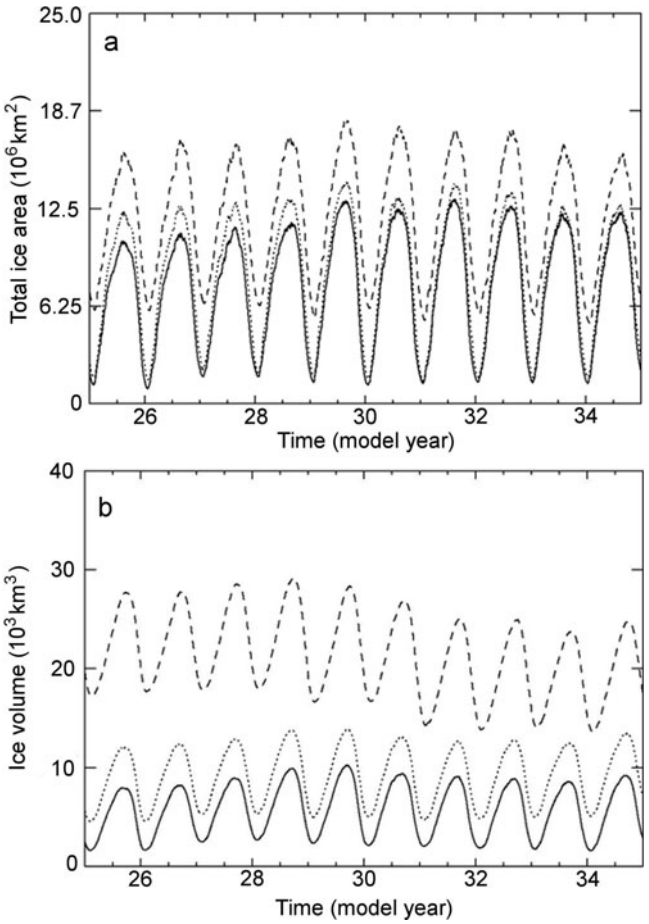

Fig. 3. Evolution of (a) total sea-ice area and (b) volume in the Southern Hemisphere over years 25–34 in the control run (solid lines), the no-shelves run (dotted lines) and the no-WAIS run (dashed lines).

requires 1–2 weeks of computational time on 32 processors of an SGI O2000 computer, parallelized using the Message Passing Interface (MPI). This simulation period appears to be sufficient to see a transient, rapid relaxation from initial conditions at the surface (Fig. 2) and to see clear differences in the Southern Ocean circulation and sea-ice conditions among the three model runs.

Selected model limitations

Because of our scientific objectives, we decided to model sea surface salinity (SSS) and temperature (SST) without restoring data as is commonly done (e.g. Goosse and others, 2001; Duffy and others, 2002; Stössel and others, 2002). As well as forcing the ocean surface environment to revert toward recent conditions, restoring would require an estimation of surface conditions in the newly exposed sub-Antarctic areas for which we do not have data. The POP–CICE model at 3° resolution does not maintain the North Atlantic thermohaline circulation for more than about 40 model years. This is a common problem of global ice–ocean models with no salinity/temperature restoration. Fully coupled climate models (that is, including a full atmospheric component) tend not to exhibit this problem, but the computational expense of running a fully coupled model to global equilibrium for each case would be at least an order of magnitude greater than the resources available for this study. Using an atmospheric mixed layer helps maintain overturning in the North Atlantic over more model years, further justifying its use.

Thus, the main limitation of this study lies in the short period of time for which we were able to run the model. Even if a full steady state cannot be ascertained with the tools at hand, it is still valuable to analyze the direction of changes observed in our experiments, keeping in mind that the absolute magnitude of these changes may be different in a steady state. Forty years is one to two orders of magnitude smaller than the timescale required to establish a full global steady state in the ocean (Duffy and others, 2002). Nevertheless, at least near the surface, the model approaches quasi-equilibrium for surface temperature and salinity, as illustrated in Figure 2. We are therefore reasonably confident that the trends we observe in our model results are valid near Antarctica. We make the common assumption that existing numerical model biases remain constant in the different numerical experiments, and that inter-comparisons between model runs are scientifically robust.

We do not include transient effects that may arise during disintegration of the West Antarctic ice shelves and ice sheet, such as an increase in freshwater flux to the ocean. Such freshwater fluxes may reach ~0.1–1.0 sverdrup (1 Sv = 0.001 km^3 s^{-1}) for fast but feasible timescales of tens to hundreds of years for ice shelf disintegration, and hundreds to thousands of years for the collapse of the WAIS. This range of freshwater fluxes is large compared with the present steady-state freshwater flux from the whole of Antarctica of 0.05 Sv, and could affect the oceanic circulation in a way that is not tested here. We also neglect the equilibrium freshening

https://doi.org/10.3189/002214307783258440 Published online by Cambridge University Press

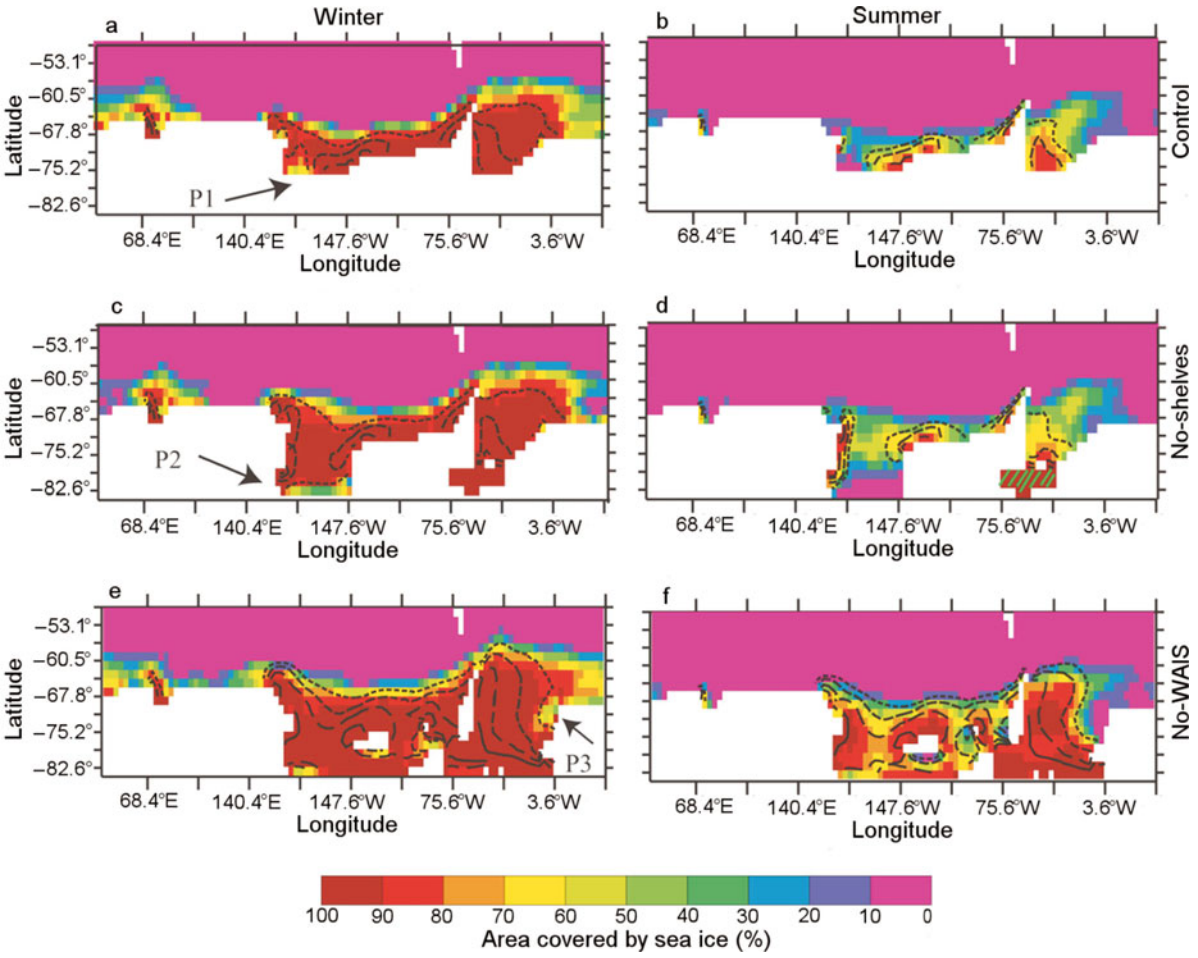

Fig. 4. Sea-ice extent and thickness, averaged over years 25–34. Winter (June–August) results are on the left and summer (December–February) on the right. Results from the control run are shown in (a) and (b), from the no-shelves run in (c) and (d) and from the no-WAIS run in (e) and (f). Contour lines indicate the sea-ice thickness distribution (dotted lines: 0.5 m; short dashes: 1 m; long dashes: 2 m; solid lines: 4 m). In the RIS sector, the polynya labelled P1 (a) is significantly wider in the no-shelves run (labelled P2 in (c)). In the FRIS sector, fast ice (green hatching) forms south of Berkner Island (no-shelves case), while a major polynya is located on the eastern side of the island in the no-WAIS run (P3 in (e)).

of the global ocean by ~0.1‰ due to permanent release of water stored currently in the WAIS. Again, the sole objective of this study is to observe model response to changes in the extent of shelf and land ice in West Antarctica.

RESULTS

To minimize the influence of year-to-year fluctuations in atmospheric boundary conditions, results are averaged over 10 years (year 25 to 34) unless otherwise specified.

Sea-ice distribution

In the two experimental runs, sea-ice concentration and thickness in West Antarctica clearly change in response to the imposed perturbation in shelf- and land-ice extent. Analysis of ice area and volume time series indicates that $>1 \times 10^6\,\mathrm{km}^2$ of additional ocean surface is covered by sea ice in winter when the ice shelves are removed (Fig. 3a). Hence, the increase in sea-ice cover is more or less equivalent to the increase in sea surface area caused by the removal of the ice shelves. However, removing the WAIS leads to extensive perennial sea-ice cover and an increase in winter sea-ice area by $5 \times 10^6\,\mathrm{km}^2$, compared with the control run. This means that the new sea-ice cover grows to about twice the size of the sea surface area generated by the disappearance of the WAIS. The Antarctic sea-ice volume increases by a factor of about 1.5 in the no-shelves experiment, while it increases about four-fold in the no-WAIS run (Fig. 3b). The seasonal variability of sea-ice volume and area is also larger in the experimental runs than in the control run.

Spatial distributions of sea-ice concentration and thickness differ in the three runs (Fig. 4). The control run develops a polynya (P1; Fig. 4a and b) in the western part of the RIS embayment. In the no-shelves run, a large polynya (P2; Fig. 4c) opens all along the southern edge of the removed RIS and sea ice formed during the winter generally melts over the summer (Fig. 4d). Fast ice builds up south of Berkner Island, in the removed-FRIS area (Fig. 4d). It is possible that the presence of Berkner Island hinders an efficient outflow of the sea ice which forms to the south of it, as suggested by the fairly slow oceanic surface circulation (not shown). However, when modifying the bathymetric grid, we ensured that the grid has an opening wide enough for the POP model to resolve the circulation. North of Berkner Island, the sea-ice seasonal variability is slightly greater compared with the control run (Fig. 4d; thinner ice, less coverage).

https://doi.org/10.3189/002214307783258440 Published online by Cambridge University Press

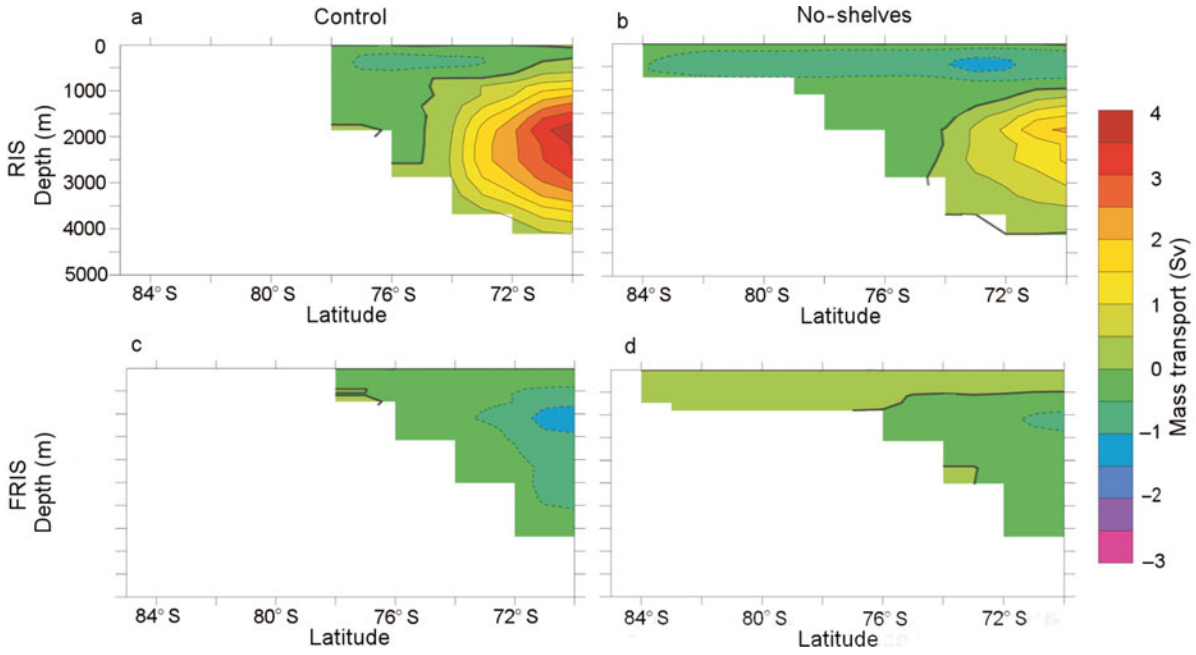

Fig. 5. The overturning stream function (Sv) averaged over model years 25–34 for the (a, b) RIS and (c, d) FRIS sectors. Control-run results are shown in (a) and (c) and for the no-shelves run in (b) and (d). The thick solid line indicates the zero contour line. Negative values designate counter-clockwise circulating cells (in a vertical plain) while positive values show clockwise circulating cells. White steps show the maximum bathymetry within each latitudinal band. The no-WAIS case is not included as it is not possible to dissociate the RIS from the FRIS areas for these calculations.

In the no-WAIS case, the extensive RIS-region polynya evident in the no-shelves case fails to open, while a new polynya opens in the eastern part of the FRIS area (P3; Fig. 4e) and next to the Antarctic Peninsula (Fig. 4e). Overall, sea-ice thickness is much greater in the no-WAIS run (~2–3 m, compared with ~1–2 m in the control and no-shelves simulations, Fig. 4), and becomes perennial over a large extent of the ocean. The summer volume of sea ice increases from ~1000–2000 km^3 in the baseline run to ~5000 km^3 in the no-shelves run and ~15 000–18 000 km^3 in the no-WAIS run.

Mass transport

The zonally averaged, meridional overturning stream function (Fig. 5) suggests that increasing the volume and area of sea ice produced at the ocean surface leads to weakening of the large circulation cell in the RIS sector and little change in the FRIS region. These changes in circulation affect distributions of temperature and salinity within the Southern Ocean, and are likely driven by the character of the sea-ice cover (a solid layer compared with open water and polynyas). In the case of no-WAIS, the Ross embayment waters are particularly fresh at the surface, while intermediate and deep waters are relatively warm. The most dense, cold and saline of all Antarctic waters is formed in the FRIS area in the no-WAIS case. When the total mass transport for the RIS and FRIS areas is averaged, the removal of the WAIS replaces the predominance of surface downwelling and deeper upwelling typical of the control run with several regional circulation cells. This development may be attributed to the fact that removal of the WAIS opens a hydrographic connection between marginal seas through the interior West Antarctic basin.

Due to the limitations discussed above, we do not dwell on the magnitude of these changes or on their global connections. However, it is interesting to note that the global overturning stream function strengthens with the modelled expansion of the sea-ice formation regions, enhancing southward heat transport toward Antarctica.

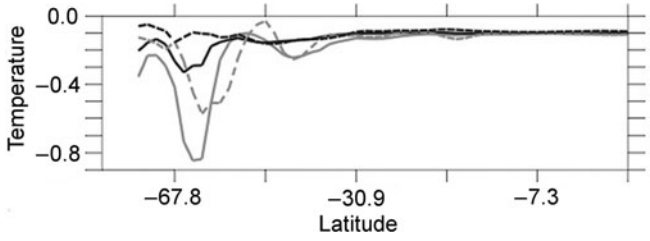

Fig. 6. Differences in Southern Hemisphere sea surface temperatures between experimental runs, averaged over model years 25–34. Data averaged across all longitudes (solid lines) are plotted in black for the difference between the no-shelves and the control run, and in grey for the difference between the no-WAIS and the control run. Dashed lines represent data that were zonally averaged across the Atlantic Ocean.

Sea surface temperatures and evaporation

Figure 6 plots the differences in sea surface temperatures between the different experiments. In both the no-shelves and no-WAIS cases, a drop in sea surface temperature is observed in sub-Antarctic latitudes. Maximum cooling is measured at ~65° S, which corresponds to the northern edge of the sea-ice cover. This cooling is more pronounced in the Indian–Pacific Ocean than in the Atlantic, probably because the new sea-ice distribution leads, in both cases, to higher rates of ice melting in the RIS area, facing the Indian–Pacific Ocean. Meltwater suppresses heat fluxes from the deeper ocean, potentially leading to a cooler sea surface (and

https://doi.org/10.3189/002214307783258440 Published online by Cambridge University Press

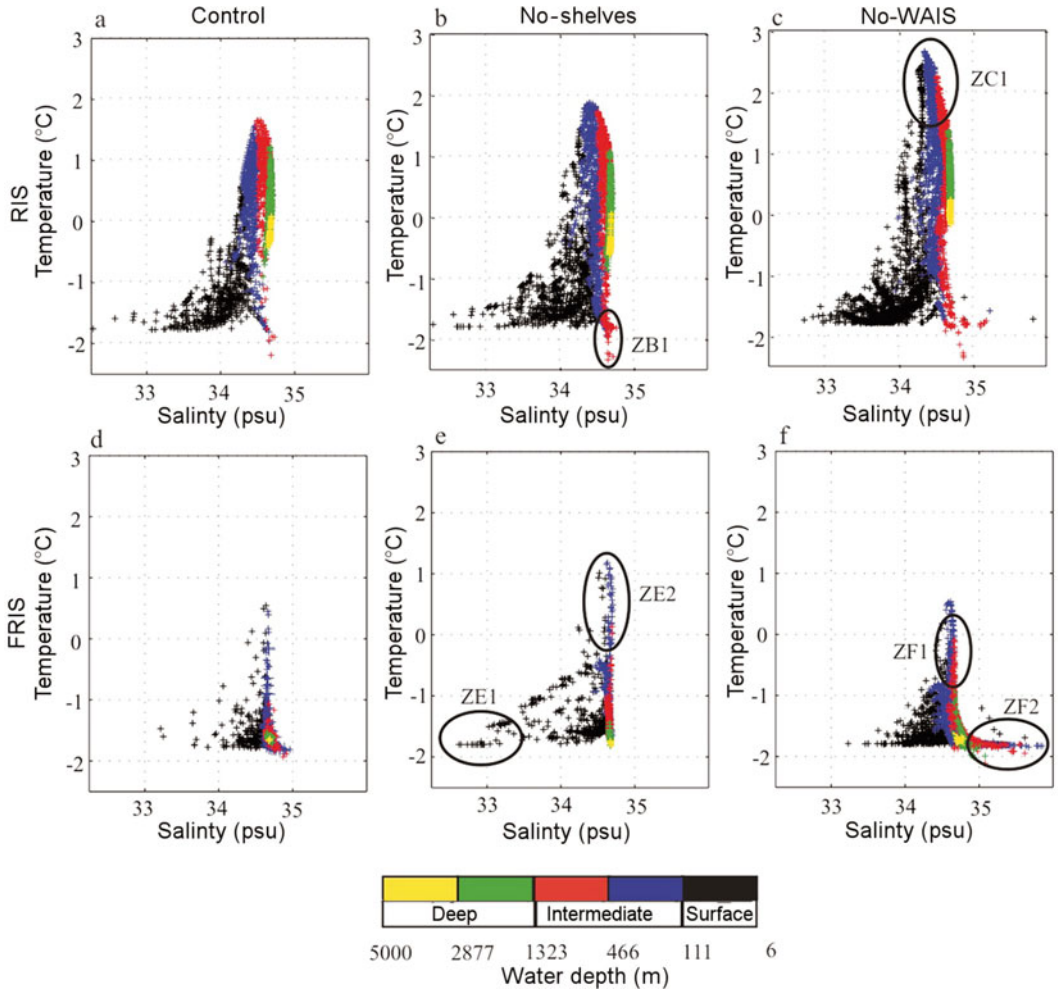

Fig. 7. Potential temperature–salinity diagrams based on data averaged over model years 25–34. (a–c) The RIS sector is bounded by 169.2° E, 64.8° W, 82.6° S and 67.8° S. (d–f) The FRIS sector is bounded by 61.2° W, 3.6° W, 82.6° S and 67.8° S. Results for the control run are shown in (a) and (d), for the no-shelves run in (b) and (e) and for the no-WAIS run in (c) and (f). From a detailed spatial analysis, we identify several zones of origin for different waters: ZB1 is the cold water produced in the polynya P2. The warm water of ZC1 accumulates beneath the perennial ice cover. ZE1 and ZE2 are the cold surface and warmer upper-intermediate waters, formed beneath the fast ice south of Berkner Island, respectively. The warmer intermediate water composing ZF1 is found beneath the thick sea-ice cover in the no-WAIS run. ZF2 corresponds to the very saline and cold water produced in the no-WAIS run within the polynya P3. The outlier points representing very cold or very saline conditions are caused by undershoots in model advection routines.

subsequently more ice). This scenario is supported by the modelled ocean circulation, discussed in the following section. It is unlikely that evaporation is causing the ocean surface to be cooler in the two sensitivity runs because the winter ice edge is further north in those cases, which would have an insulating effect. In fact, plots of evaporation (not shown) illustrate that evaporation drops to near zero in areas of sea-ice cover.

Another notable feature of Figure 6 is that sea surface temperatures north of ~40° S differ between runs by <0.1°C. This illustrates the reproducibility of results away from the source of the imposed changes in ice extent in West Antarctica.

Temperature, salinity and density

Temperature–salinity diagrams for FRIS and RIS embayments are shown in Figure 7. Analysis of these panels provides an insight into how the new sea-ice distribution associated with landmask modifications affects the oceanic water mass properties. Partly guided by the depths of boundaries between layers in the ocean model, we define surface water as 0–111 m deep; intermediate water as 111–1323 m deep; and deep water as 1323–5000 m deep.

No-shelves experiment

In the removed-RIS area, cold and saline water forms in the southern part of the Ross embayment (zone ZB1; Fig. 7b). This is due to the combined effect of the large polynya P2 and the high seasonal variability of sea-ice cover. The resulting dense water sinks to the sea bottom and flows to the east (not shown). This downwelling may be responsible for weakening by half of the deep meridional stream-function cell in the no-shelves run compared with the control run (Fig. 5a and b). At the same time, cold surface water (here <0°C) appears at the northern limit of the polynya and reaches 64.2° S, while the same surface isotherm is located around 66° S in the control run (Fig. 8a and b). At the sea-ice edge, this cold surface water is also fresher by up to 0.3 psu than in the control run. In summer, a greater volume of sea ice melts in lower latitudes and results

https://doi.org/10.3189/002214307783258440 Published online by Cambridge University Press

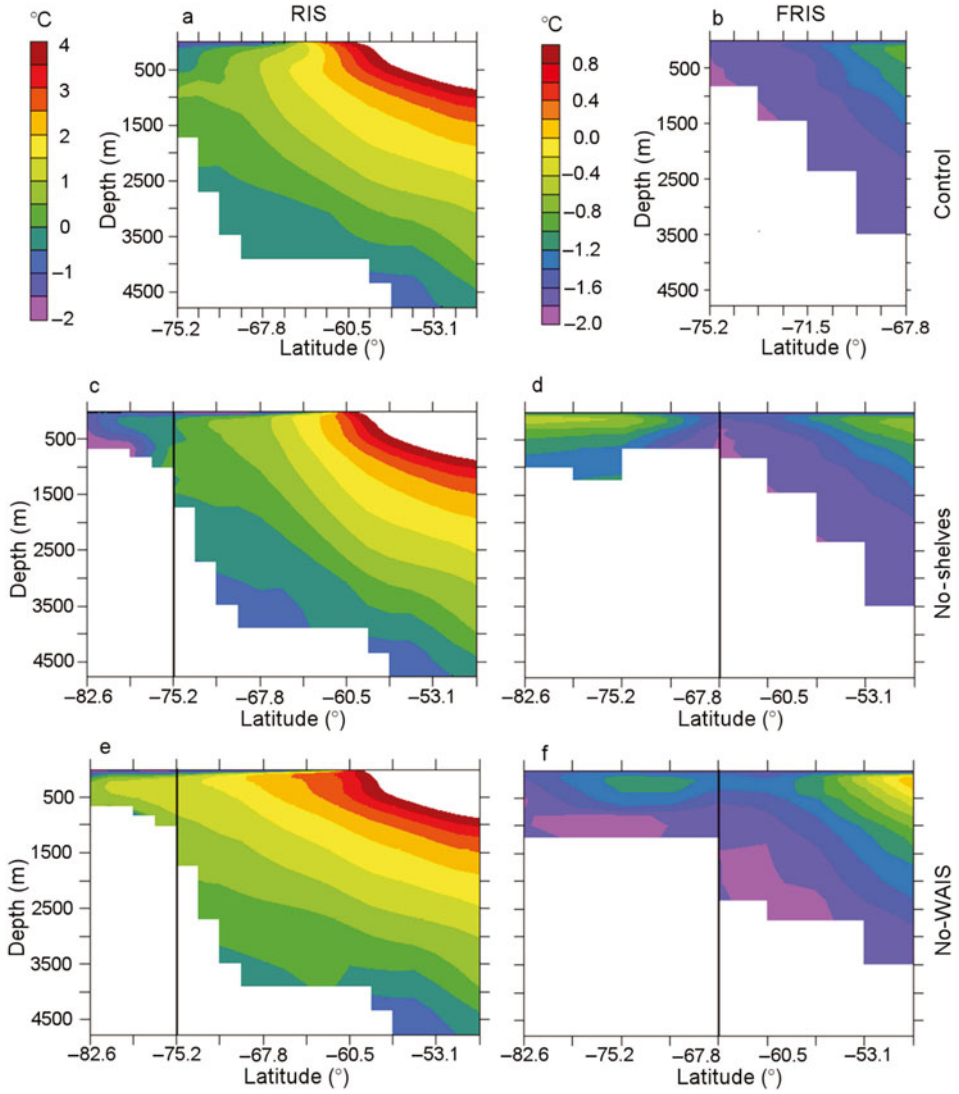

Fig. 8. Ocean temperature time-averaged over model years 25–34 and zonally averaged for the RIS (a–c) and FRIS (d–f) sectors (white boxes in Fig. 1) for the three model runs.

in high surface freshwater flux. Below this fresh and cold surface water, warmer water penetrates southward, but the polynya cools the sea water so efficiently that the overall temperature at intermediate depth is lower than in the control case (Fig. 7b). A detailed analysis of the relative changes of density indicates that modification of the sea-water density mostly reflects the salinity changes at the surface (lower salinity of the surface at lower latitudes and increased salinity at polynya P2) and changes in temperature at depth (colder than in the control run).

In contrast, in the FRIS embayment (Fig. 7e) the build up of fast ice insulates the ocean thermally. As a result, the upper oceanic layer (zone ZE1, Fig. 7e) is fresher (salinity is 1 psu lower than north of Berkner Island) whereas deep and intermediate waters are up to 0.6°C warmer than water found north of the island (zone ZE2; Fig. 7e). In the Weddell Sea, the intermediate and deep water tends to warm slightly (~0.2°C). Density of the whole sea-water column within the FRIS embayment (south of Berkner Island; zones ZE1 and ZE2) is lower than that to the north. This configuration is not seen in the other experiments and leads to weak upwelling near the surface and weakened downwelling at depth (Fig. 5d).

No-WAIS experiment

In this experiment, much of the RIS embayment is capped by a perennial sea-ice cover and does not fill with cold water as observed in the no-shelves run. As with the FRIS embayment in the no-shelves experiment, this ice cover hinders heat loss from this part of the ocean, and ocean circulation extends the effect of this warming beyond the northern boundary of sea-ice cover. Hence, the intermediate and deep ocean waters north of the embayment are up to 1°C warmer than in the control run (zone ZC1; Figs 7c and 8). The minimum deep-water temperature does not drop below –0.2°C (Fig. 7c), contrasting with –1°C in the control and no-shelves simulations (Figs 7a, b and 8). This penetration of warm water leads to a strong thermal stratification. The surface mixed layer is close to the freezing point, and lies above waters that are 3–4°C warmer (Fig. 7c). Moreover, this thermal stratification extends 250 km further north compared with the control run (Fig. 8). Hence, the RIS sector experiences quite different oceanographic conditions in the no-WAIS experiment (Fig. 7c) compared with the no-shelves run (Fig. 7b), mainly because a perennial ice cover fills the embayment and the extensive polynyas seen in the no-shelves simulation are not

https://doi.org/10.3189/002214307783258440 Published online by Cambridge University Press

present. In spite of the strong thermal stratification with cold water above warm water, the density stratification remains stable, as the surface mixed layer is also much fresher than the water below (Fig. 7c). It is unlikely that the system would become unstable, as only an increase in salinity could trigger this. Since the sea ice covering the RIS area is mostly perennial, brine production in the experiment is also limited.

In the no-WAIS run, the intermediate water beneath the FRIS area warms by up to 1°C compared with the control run (zone ZF1; Figs 7f and 8). The temperature is not as high as in the removed RIS area because the sea ice is not as thick in the FRIS embayment as in the RIS embayment (Fig. 4e and f). The high salinity water (zone ZF2; Fig. 7f) is associated with polynya P3, and to a lesser extent the southwest area of the FRIS. This water appears to be the densest of all sub-Antarctic waters and should lead to increased downwelling in this region.

DISCUSSION AND CONCLUSIONS

Our numerical experiments suggest that increased exposure of ocean surface to sea-ice formation in West Antarctica modifies thermohaline structure and circulation in the Southern Ocean. The primary consequence of opening additional polar sea surface area in West Antarctica is an increase in sea-ice production and a northward advance of the sea-ice cover. Whereas seasonal variability remains large in the two experimental runs, most of the additional sea ice forming in the no-WAIS run becomes perennial.

Several features of our results are particularly noteworthy in the light of the current discussions about future and past evolution of Antarctic ice sheet and climate. First, within just several dozens of model years, the output from our experimental runs (no-shelves and no-WAIS) differed from the control run, at least in the Southern Hemisphere. Second, there is a non-linearity in the response of ocean surface condition and ocean circulation to the introduced perturbations. As the portion of the West Antarctic region exposed to sea-ice formation increases, from the control to the no-shelves and the no-WAIS case, there are notable shifts in the location of major upwelling and downwelling zones as well as in the location of large polynyas. Furthermore, the removal of the WAIS enhances southward penetration of relatively warm intermediate waters beneath the increased sea-ice cover. Elevated heat transport southward may hinder rebuilding of the WAIS in case of its disappearance and could increase mass loss from those parts of the East Antarctic ice sheet that would become exposed to the West Antarctic intermediate waters. Since expansion of sea-ice cover cuts down on evaporation from the marginal seas, remaining Antarctic ice masses may also experience decreased snow accumulation due to shrinkage of shelf and land ice in West Antarctica.

Our results suggest sensitivity of oceanographic conditions in the Southern Ocean to changes in West Antarctic ice extent, as the oceanic mass and heat transport are affected even in relatively short model runs. Clear differences occur among the three reported model runs despite the fact that the imposed landmask modifications affect <0.6% of global ocean area. Although further numerical investigations are needed to fully evaluate the possible spectrum of impacts that changes in the extent of West Antarctic ice shelves and ice sheet may have on the global ocean, our results support previous work attributing an important role to Antarctic circulation in global climate change (Seidov and others, 2001; Weaver and others, 2003).

ACKNOWLEDGEMENTS

This work was supported by a grant from the IGPP/LANL-UC collaboration program to E. Hunke and S. Tulaczyk. We gratefully acknowledge M. Maltrud (LANL) and M. Hecht (LANL) for their help configuring the ocean model and assembling river runoff data. We also thank R. Anderson and G. Glatzmaier for helpful comments on early versions of this manuscript.

REFERENCES

Bentley, C.R. 1997. Rapid sea-level rise soon from West Antarctic ice sheet collapse? *Science,* **275**(5303), 1077–1078.

Bentley, C.R. 1998. Rapid sea-level rise from a West Antarctic ice-sheet collapse: a short-term perspective. *J. Glaciol.,* **44**(146), 157–163.

Best, S.E., V.O. Ivchenko, K.J. Richards, R.D. Smith and R.C. Malone. 1999. Eddies in numerical models of the Antarctic circumpolar current and their influence on the mean flow. *J. Phys. Oceanogr.,* **29**(3), 328–350.

Bindschadler, R. 1997. Letters. West Antarctic ice sheet collapse? *Science,* **276**(5313), 662–663.

Bindschadler, R. 1998. Future of the West Antarctic ice sheet. *Science,* **282**(5388), 428–429.

Blackmon, M. *and 25 others*. 2001. The community climate system model. *Bull. Am. Meteorol. Soc.,* **82**(11), 2357–2376.

Duffy, P.B., M.E. Wickett and K. Caldeira. 2002. Effect of horizontal grid resolution on the near-equilibrium solution of a global ocean–sea ice model. *J. Geophys. Res.,* **107**(C7), 3075. (10.1029/2000JC000658.)

Goosse, H. and T. Fichefet. 1999. Importance of ice–ocean interactions for the global ocean circulation: a model study. *J. Geophys. Res.,* **104**(C10), 23,337–23,355.

Goosse, H., J.-M. Campin and B. Tartinville. 2001. The sources of Antarctic bottom water in a global ice–ocean model. *Ocean Model.,* **3**(1–2), 51–65.

Hunke, E.C. and W.H. Lipscomb. 2001. *CICE: the Los Alamos sea ice model documentation and software user's manual.* Los Alamos, NM, Los Alamos National Laboratory.

Levitus, S., R. Burgett and T.P. Boyer. 1994a. *World ocean atlas 1994. Vol. 3. Salinity.* Washington, DC, US Department of Commerce. National Oceanic and Atmospheric Administration. (NOAA Atlas NESDIS 3.)

Levitus, S., T.P. Boyer and J. Atonov. 1994b. *World ocean atlas 1994. Vol. 4. Temperature.* Washington, DC, US Department of Commerce. National Oceanic and Atmospheric Administration. (NOAA Atlas NESDIS 4.)

Lythe, M.B., D.G. Vaughan and BEDMAP consortium. 2001. BEDMAP: a new ice thickness and subglacial topographic model of Antarctica. *J. Geophys. Res.,* **106**(B6), 11,335–11,351.

McClean, J., M.E. Maltrud and A.J. Semtner. 1997. Comparison of the LANL POP model and observations in the South Atlantic. International WOCE Newsletter, 28. World Ocean Circulation Experiment.

Oppenheimer, M. 1998. Global warming and the stability of the West Antarctic ice sheet. *Nature,* **393**(6683), 325–332.

Prasad, T.G., J.L. McClean, E.C. Hunke, A.J. Semtner and D. Ivanova. 2005. A numerical study of the western Cosmonaut polynya in a coupled ocean–sea ice model. *J. Geophys. Res.,* **110**, C10008. (10.1029/2004JC002858.)

Scherer, R.P., A. Aldahan, S. Tulaczyk, G. Possnert, H. Engelhardt and B. Kamb. 1998. Pleistocene collapse of the West Antarctic ice sheet. *Science,* **281**(5373), 82–85.

https://doi.org/10.3189/002214307783258440 Published online by Cambridge University Press

Seager, R., M.B. Blumenthal and Y. Kushnir. 1995. An adjective atmospheric mixed layer model for ocean modeling purposes: global simulation of surface heat fluxes. *J. Climate,* **8**(8), 1951–1964.

Seidov, D., E. Barron and B.J. Haupt. 2001. Meltwater and the global ocean conveyor: northern versus southern connections. *Global Planet. Change,* **30**(3–4), 257–270.

Smith, R.D., J.K. Dukowicz and R.C. Malone. 1992. Parallel ocean general circulation modeling. *Physica D,* **60**(1–4), 38–61.

Stössel, A., K. Yang and S.J. Kim. 2002. On the role of sea ice and convection in a global ocean model. *J. Phys. Oceanogr.,* **32**(4), 1194–1208.

Weaver, A.J., O.A. Saenko, P.U. Clark and J.X. Mitrovica. 2003. Meltwater pulse 1A from Antarctica as a trigger of the Bølling-Allerød warm interval. *Science,* **299**(5613), 1709–1713.

Xie, P. and P.A. Arkin. 1996. Analyses of global monthly precipitation using gauge observations, satellite estimates, and numerical model predictions. *J. Climate,* **9**(4), 840–858.

MS received 12 September 2006 and accepted in revised form 29 March 2007